Overview of VLBI instrument for Millimetron space mission

A. Khudchenko, A. Smirnov, S. Turygin, M. Andrianov, V. Kostenko, et al.

A. Khudchenko, A. Smirnov, S. Turygin, M. Andrianov, V. Kostenko, A. Baryshev, E. Golubev, R. Cherny, A. Andrianov, A. Ozolin, I. Tretyakov, M. Arkhipov, V. Koshelets, R. Hesper, S-T. Han, J-W. Lee, T. Jung, A. Rudnitskiy, S. Likhachev, "Overview of VLBI instrument for Millimetron space mission," Proc. SPIE 12190, Millimeter, Submillimeter, and Far-Infrared Detectors and Instrumentation for Astronomy XI, 121902W (31 August 2022); doi: 10.1117/12.2630728

Event: SPIE Astronomical Telescopes + Instrumentation, 2022, Montréal, Québec, Canada

Overview of VLBI instrument for Millimetron space mission

A. Khudchenko*[a], A. Smirnov[a], S. Turygin[b], M. Andrianov[a], V. Kostenko[a], A. Baryshev[c], E. Golubev[a], R. Cherny[a], A. Andrianov[a], A. Ozolin[a], I. Tretyakov[a], M. Arkhipov[a], V. Koshelets[a,d], R. Hesper[c], S-T. Han[e], J-W Lee[e], T. Jung[e], A. Rudnitskiy[a], S. Likhachev[a],
[a]Astro Space Center of P.N. Lebedev Physical Institute, Leninskyi prospect 53, 199911, Moscow, Russia; [b]FGUP SKB of Institute of Radio Engineering and Electronics, Vedenskogo 4, 141190, Fryazino, Russia; [c]Kapteyn Astronomical Institute, University of Groningen, Lnadeven 12, 9747 AD, Groningen, Netherlands, [d]V.A. Kotel'nikov Institute of Radio engineering and Electronics RAS, Mokhovaya 11/7, 125009, Moscow, Russia; [e]Korea Astronomy and Space Science Institute, Daedeokdae-ro 776, Yuseong-gu, Daejeon 34055, Republic of Korea

ABSTRACT

Millimetron space observatory will be equipped with the cryogenically cooled instruments for a Space-Earth Very Large Baseline Interferometry (S-E VLBI). It will be a heterodyne multichannel receiver including 7mm, 3mm, 1.3mm and (presumably) 0.8mm channel. Two low frequency channels will be based on HEMT amplifiers, while for the high frequencies superconductor-insulator-superconductor (SIS) receivers will be utilized. The VLBI instrument will have a multi frequency capability allowing simultaneous observation using several channels. This mode has a high potential for improving of black hole event horizon observations due to phase transferring capabilities. The multi frequency observation will be provided by a signal split in the input optics and by back-end capabilities.

Keywords: Interferometry, VLBI, receivers, high rate data transfer.

1. INTRODUCTION

The most recent Space-Earth Very Large Base Interferometry (S-E VLBI) has been implemented in a space mission Radioastron. It was a 10 meter space radiotelescope, that has been successfully operating for more than seven years [1]. The operation frequency of Radioastron was up to 22 GHz. The results of Radioastron and the recent achievements of Event Horizon Telescope (EHT) project [2,3] show a unique potential of possible S-E VLBI system observing in mm range of wavelength. Millimetron space observatory with a prime mirror of 10m in diameter is dedicated for this task. The mission of it is to study metrics of supermassive black holes, the environment close to them [4] and potentially approach the question of existence of the wormholes. Millimetron space observatory will operate in halo orbit around Lagrangian point L2 of the Sun-Earth system. Halo orbit is a quasi-stable orbit, located in the vicinity of L2 point in the plane perpendicular to the ecliptic one. Within the joint EHT and Millimetron program an expected imaging resolution at 230 GHz can reach $\Delta\theta \sim 5$ µas [4].

Millimetron S-E VLBI receivers will be used for interferometric observations between Millimetron and ground stations such as ALMA, NOEMA, EHT network, KVN network and so on. For efficient operations, VLBI instruments of Millimetron are split into frequency bands, matching those of ALMA and other ground based stations. The future plans of EHT project clearly show the interest to extend the telescope network and probe the observations not only at 230 GHz, but also in the next atmospheric window at 345 GHz [5]. This makes a very strong motivation to have VLBI receivers for these bands onboard of Millimetron.

*khudchenko@asc.rssi.ru; phone +7 926 379-0391;

Millimeter, Submillimeter, and Far-Infrared Detectors and Instrumentation for Astronomy XI, edited by Jonas Zmuidzinas, Jian-Rong Gao, Proc. of SPIE Vol. 12190, 121902W · © 2022 SPIE · 0277-786X · doi: 10.1117/12.2630728

2. GENERAL DESCRIPTION OF THE MILLIMETRON VLBI RECEIVER SET

2.1 Space-Earth interferometer

Ones we are talking about capabilities of an interferometer one should take into account all the parts including stations, receivers, data processing and the way it is delivered to the correlator. A simplified block diagram for the case of Space-Earth Interferometer with Millimetron as a space station can look as shown in Figure 1. The key features of this system are the following: 1) the space observatory will be Millimetron with a prime mirror of 10 m in diameter with a surface quality rms = 6 μm; 2) ground based stations set is expected to be similar to a new generation of Event Horizon Telescope (ngEHT) [5]; 3) space station will be orbiting around L2 point [4]; 4) the onboard receivers set will be as similar as possible to the ground facilities including 7mm, 3mm, 1.3 mm and 0.8 mm channels; 5) the onboard clock will be based on a hydrogen maser; 6) Millimetron will have a capability of multi-frequency observations; 7) Millimetron data will be transferred to Earth using high data rate line and delivered to a correlator.

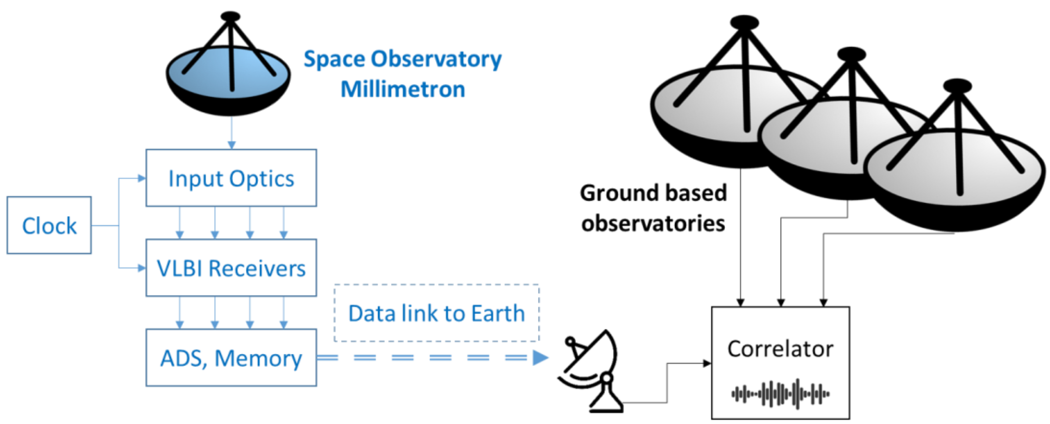

Figure 1. A simplified block diagram of the Space-Earth Interferometer.

2.2 S-E VLBI instrument interferometer

A detailed block diagram describing the onboard S-E VLBI receiver set with supplementary systems is shown in Figure 2. This diagram shows schematically all the main functional modules participating in the signal processing. Input signal will be split by three dichroics to feed all 4 channels in parallel. The details of an optical design will be described below in this paper. Later, the four receivers realize the down-conversion of the detected signals to an intermediate frequency (IF) of 4-12 GHz. These signals are transformed in an IF module to four baseband signals of 4 GHz BW. The IF module with commutation block allows to connect any receiver output to any on four ADC inputs. The ADC unit can process 4 channels of 4 GHz BW baseband for further storing in array of Formators. The stored data will be sent to Earth using a high data rate connection line.

The onboard clock is based on hydrogen maser. The clock unit generates a reference signal of 100 MHz utilized to synchronize generators in the local oscillator unit. This unit produces a set of high frequency signals, which are used as local oscillator (LO) signals in all the VLBI receivers either directly or after frequency multipliers. The frequency multipliers used for two higher frequency receivers are shown out of the the Local Oscillator Unit, because they are planed be located outside at lower temperature to minimize the LO noise contribution in the receiver noise temperature.

The block diagram shows for convenience the corresponding temperature levels of the units.

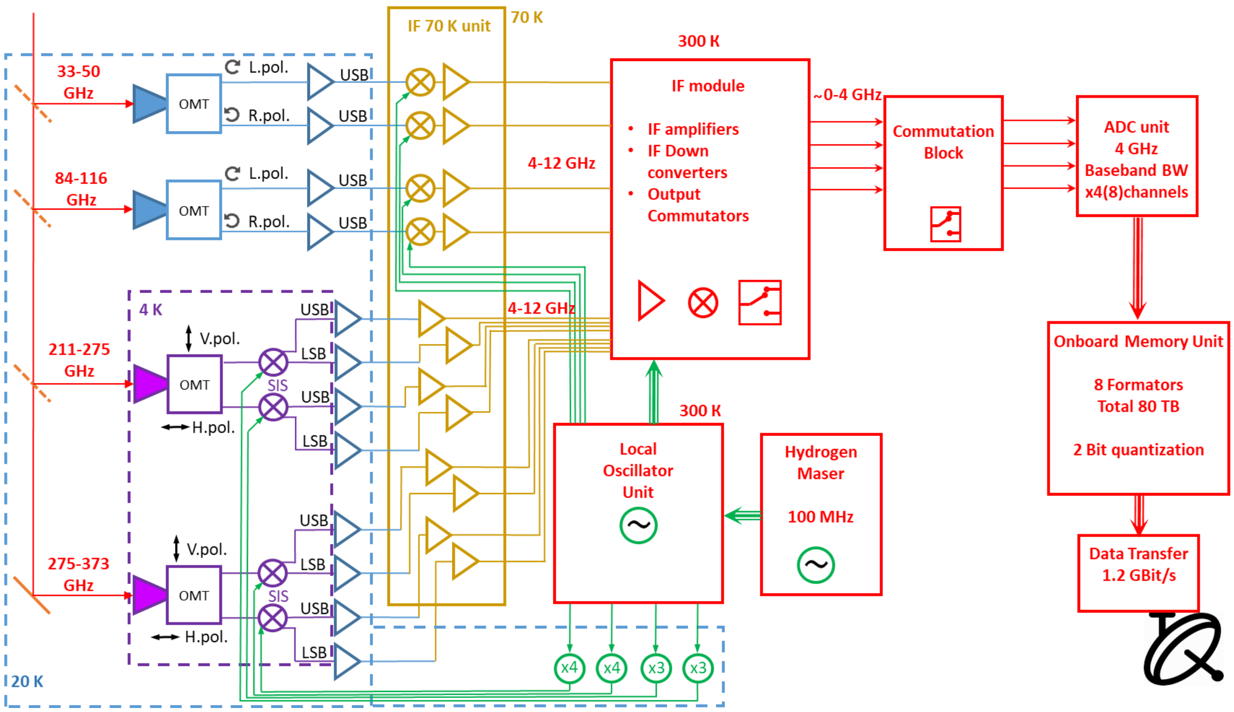

Figure 2. Block diagram of the Millimetron Space-Earth receivers with supplementary systems.

2.3 Receivers

The Millimetron VLBI instrument will include a number of receivers corresponding to frequency bands common for ground based telescopes. For the moment, it is decided to install three receivers for frequency ranges 33-50 GHz, 84-116 GHz and 211-275 GHz. There is a very strong scientific motivation to have also the 4th receiver operating in frequency range 275-373 GHz. This channel is included already in design work, particularly in optical layout, but official decision is still in process. In addition to Figure 2, Table 1 describes the main parameters of the Millimetron VLBI receivers. The required sensitivity of the receivers is presented in a way similar to ALMA standard, i.e. using specification for 80% and for 100% of a band. Receivers VLBI-1 and VLBI-2 will utilize HEMT amplifiers as the first stage. Herewith, channels VLBI-3 and VLBI-4 will be based on superconductor-insulator-superconductor (SIS) mixers, state-of-the-art technology in terms of sensitivity for frequencies above 150 GHz. All the receivers will be equipped by orthomode transducers (OMT) splitting detected radiation it two polarizations (either circular or linear ones). The band VLBI-1 and VLBI-2 will detect only the upper sideband (USB), while the bands VLBI-3 and VLBI-4 will have capability to receive both sidebands USB and LSB.

Table 1. S-E VLBI receivers table.

Channel	**F, GHz**	**Tn_rec spec 80% (goal), K**	**Tn_rec spec 100% (goal), K**	**Sideband**	**Pol**	**IF range, GHz**	**Total IF BW spec (goal), GHz**	**Tech.**
VLBI-1	33-50	20 (8)	30 (12)	USB	2, circ	4-12	16	HEMT
VLBI-2	84-116	40 (32)	60 (45)	USB	2, circ	4-12	16	HEMT
VLBI-3	211-275	50 (40)	80 (64)	USB, LSB	2, lin	4-12	16 (32)	SIS
VLBI-4	275-373	60 (50)	95 (80)	USB, LSB	2, lin	4-12	16 (32)	SIS

The mixer for the channel VLBI-3 is currently under development in Astro Space Center in collaboration with Institute of Radio engineering and Electronics and Kapteyne Astronimical Institute. Recently, it was shown a prove of concept for a single-ended an SIS mixer demonstrating the double-sideband noise temperature approaching 20 K level [6],[7]. Those mixers have Nb-AlOx –Nb tunnel junctions and embedding circuit made out of Nb. For the best possible sensitivity of the Space-Earth interferometer the onboard receiver should have the same sideband configuration as the receivers installed in the ground telescopes [8], i.e. it should be sideband separating (2SB) one. Figure 3 (left) demonstrates the 3D model of RF part of the 2SB mixer equipped with two DSB mixers and a waveguide split-block. The waveguide structure contains specially designed low reflection RF hybrid, -16 dB LO couplers, LO splitter and a set of loads to dump the reflected signals.

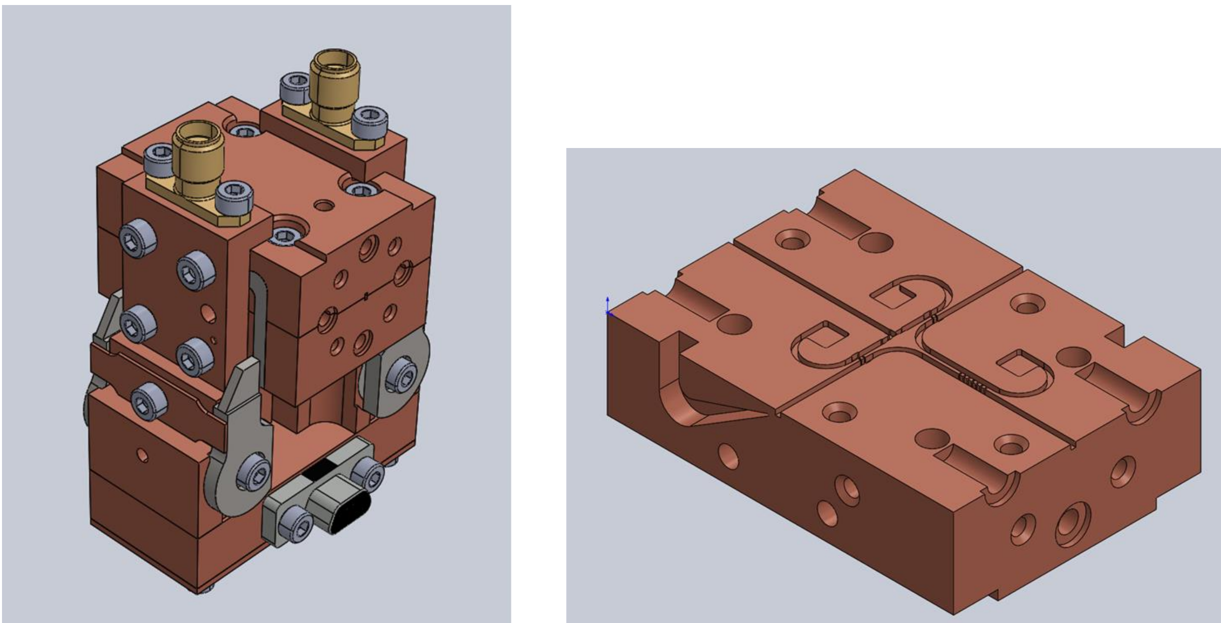

Figure 3. 3D model of the modular waveguide mixer block of the 2SB receiver 211-275 GHz. Left site figure shows the mixer RF assembly including the waveguide block, mixer holders, block with magnet coils for the critical current suppression in SIS junctions. On the right there is depicted a half of the waveguide split-block including the RF hybrid, LO couplers, LO splitter and the loads.

2.4 Sensitivity of the Space-Earth Interferometer

To estimate the possible scientific outcome of the S-E VLBI system we have calculated an expected sensitivity. Here, we have adopted the new generation of the Earth Horizon Telescope (ngEHT) configuration as it is described in [5] as a ground-based part of interferometer. The remote arm of interferometer within the framework of the Millimetron project is represented by the antenna of 10 m in diameter with a surface quality rms = 6 μm.

For simplicity, in our calculations we take ngEHT as current EHT plus a set of 30 new antennas of diameter 30 m with a moderate surface quality (σ = 65 μm). For sensitivity of the Millimetron VLBI receivers we use the numbers shown in Table 1. The noise temperature is taken from a column "Tn_rec spec 80%". Important to note, that the calculation is performed only for one polarization. The corresponding BW is 8 GHz. To assess the sensitivity of VLBI on mm-Earth baselines, we will follow the principles generally accepted in the VLBI.

The important parameter of the radio telescope is the system equivalent flux density SEFD [2]:

$$SEFD = 2k_b * T_{sys}/ A_{eff} = 2760*T_{sys}/A_{eff} \quad [Jy], \tag{1}$$

here A_{eff} is the effective area of the antenna aperture; T_{sys} – radio telescope system temperature.

The effective area is calculated using the formula:

$$A_{eff} = A_g \; *n* K_{eff} * K_{Ruze}, \tag{2}$$

here, A_g - antenna geometrical area; n - the number of antennas in the individual antenna system; Keff – the coefficient of blockage losses by the antenna structure the shading of the structure and the characteristics of the irradiation of the mirror (on average for high-quality antennas Keff =0.75); K_{Ruze} – the coefficient of loss due to the quality of the mirror. The coefficient K_{Ruze} is determined by the traditional Ruze formula:

$$K_{Ruze} = \exp(-(\frac{4\pi\sigma}{\lambda})^2)\,, \tag{3}$$

here σ is the rms surface roughness for a specific wavelength λ.

The radio telescope system temperature is estimated as $T_{sys} = (T_{rcw} + T_a)$, here T_{rcw} is the receiver noise temperature (see Table 1) and T_a is an antenna temperature, includes radiation from the external sources (for example, cosmic microwave background T_{cmb} = 2.7 K and antenna radiation losses outside the main lobe of the radiation pattern.

To calculate SEFD for a system of n individual antennas (antenna array), we use the expression [3]:

$$SEFD_{tot} = \eta_{ph} * (\sum_1^n 1/SEFD_i)^{-1} \tag{4}$$

Where η_{ph} is the phasing loss of the antenna array; for example, for the ALMA array [9,10] $\eta_{ph} \approx 0.9$.

Then the fluctuation sensitivity in terms of flux density for a ground-space interferometer of a ground-based group of EHT radio telescopes ngEHT and the MM radio telescope with a 10 m mirror on board the Millimetron observatory can be obtained from the expression:

$$dS = \frac{\sqrt{SEFD_{EHT} * SEFD_{MM}}}{\eta_c * \sqrt{BW * \tau}} \tag{5}$$

where $SEFD_{EHT}$ is calculated using (2), η_c - the correlator loss factor (0.88 with 2-bit quantization of the signal); BW – signal bandwidth, (Hz). The total bandwidth was taken into account as 2 channels USB+LSB=4+4 (GHz) in each of the 2 orthogonal polarizations; τ - the time constant (sec), which is listed below in Table 2. It is assumed that the use of the phase correction methods of the visibility function (phase correction for multi-frequency observations [11] and water vapor radiometers at ground stations [12]) will increase the integration time at high frequencies up to hundreds or tens of seconds:

The equivalent diameter of ngEHT calculated using A_{eff} and Ruze formula we estimate to be 133m, which consists of current EHT with equivalent diameter of 121m and new dishes as described above.

The results of sensitivity calculations for the interferometer Millimetron - ngEHT are shown in the Figure.4.

Table 2. Time constant for different frequencies.

Freq, GHz	43	90	230	345
τ, sec	360	250	120	60

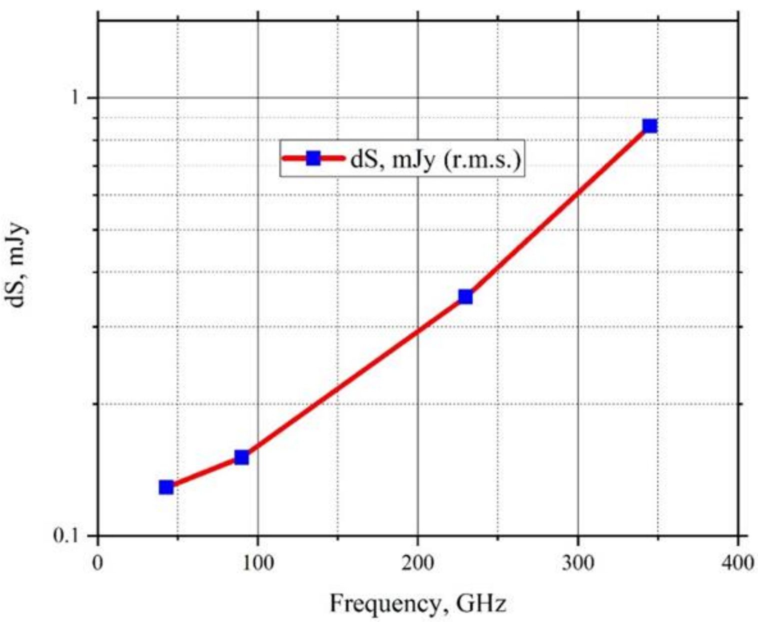

Figure 4. Sensitivity of S-E VLBI interferometer versus frequency (43, 90, 230, 345 GHz). Here, the ground part consists of the new generation EHT net and the space branch is represented by Millimetron.

3. OPTICAL LAYOUT

In millimeter-wavelength VLBI observations, the atmospheric coherence time and observation sensitivity are severely limited by the rapid tropospheric fluctuations. A multi-frequency receiving system however is capable of compensating phase errors effectively by transferring phase solutions derived from lower frequencies to higher ones based on the non-dispersive characteristic of the neutral troposphere [13]. It has been well demonstrated with the Korean VLBI Network [11],[14],[15]. Multi-frequency capability can enhance phase retrieval in VLBI observations involving a baseline with any space observatory as such system will help better determination of phase solution in case of orbital errors of the spacecraft, that are similar phase errors from the troposphere in ground observatories.

In designing optical layout for simultaneous observations of the planned RF bands, three quasi-optical low-pass filters are employed as such filters have been successfully proven for multi-frequency observations at ground millimeter VLBI observatories. In every optical train at each band are two ellipsoidal mirrors to locate the filters at the focused region for compact size. The mirrors are configured to fold the beam in zig-zag fashion to reduce total cross-polar component produced in the chain of off-axis mirrors giving no higher than -30 dB. Separations and angles between the components in the optical chain were determined using QUAST package of GRASP to give 12 dB edge taper at the subreflector as shown in Figure 5. Some beams of horns can be folded downwards to avoid interferences with other horn and to facilitate connection of the receiver components to the cold plate at the bottom of the cryogenic container.

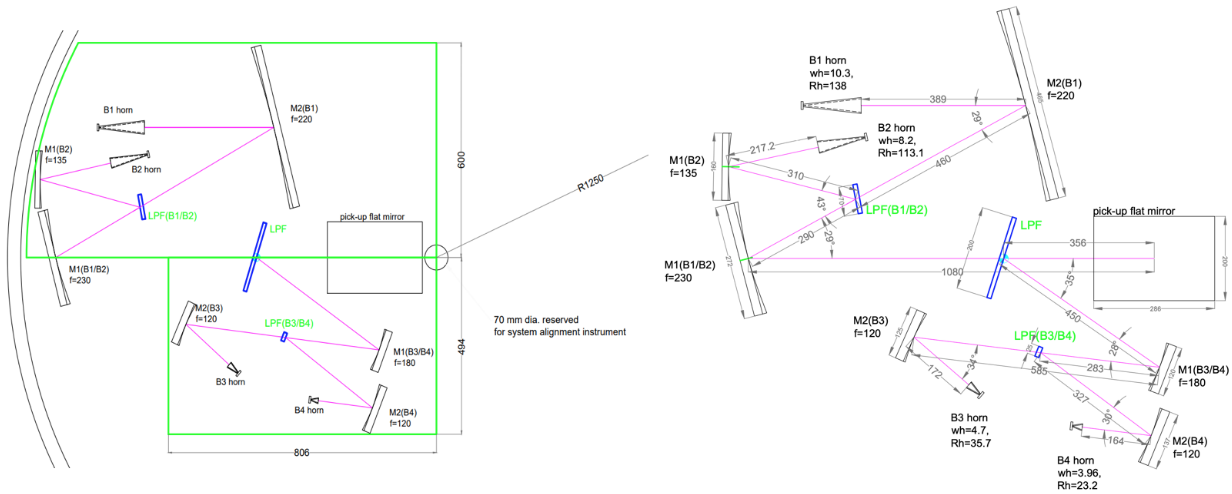

Figure 5. Top view of the planned optical layout in the cryogenic container for multi-frequency simultaneous observation (left) and its detailed dimensions (right). VLBI bands are termed as B1, B2, B3, and B4 in order of frequency ranges. All linear dimensions are in millimeters.

4. THERMAL BUDGET

The planed onboard cooling budget available for the instruments is expected to be about 500mW at 20 K level and around 100mW at 4 K stage. From the diagram in Figure 2 one can see that for the SIS receivers only the mixer part will be located at the 4 K level, while the IF amplifier will be put on the 20 K stage. The active power dissipation of the SIS mixers is way below 1 mW because of low bias currents of SIS junctions (tens of μA) and due to utilization of superconducting coils to generate magnetic field for suppression of the Josephson current. This way the heat load at 4 K level is minimized and simultaneous operation of all VLBI receivers become more feasible.

The estimations of the cooling budget required for S-E VLBI instrument are the following: 1) VLBI_1 cannel - power dissipation at 20K level: 30mW (active) plus 20mW (cabling); 2) VLBI_2 cannel - power dissipation at 20K level: 30mW (active) plus 20mW (cabling); 3) VLBI_3 cannel - power dissipation at 20K level: 20mW (active) plus 40mW (cabling), and power dissipation at 4K level: 20mW (cabling) plus 10mW (holders); 3) VLBI_4 cannel - power dissipation at 20K level: 20mW (active) plus 40mW (cabling), and power dissipation at 4K level: 20mW (cabling) plus 10mW (holders). In total the load at 4K is expected to be about 60mW and at 20K – within 220mW. Comparing these numbers with the available cooling power we conclude, that multi-frequency observations involving all four Millimetron S-E VLBI receivers are possible.

In addition, there is a room for reduction of the heat dissipation multi-frequency observations. In parallel regime it can be used only 4 GHz of BW for every receiver due to limited IF processing capabilities. This means, for example, that only one of four cryogenic IF amplifiers of the 230 GHz receiver will be used, and the others can be switched off.

5. ONBOARD DATA STORAGE

IF output signals of receivers connected through IF switching block to 8 Formators (digitization and storage devices). Each Formator has input for 4 GHz BW baseband signal. The switching block converts IF signals to 4 GHz baseband signals and is supposed to provide any combination needed for multi-frequency observations requested by science case.

Each Formator provides 8 GSPS analog-to-digital conversion with =>8 bit resolution and 2-bit resolution storage of equalized and formatted data in internal 10TB Flash memory, resulting in 16 Gigabit/sec recording rate.

The onboard data storage system consists of Formator internal FLASH memory, resulting in 80TB total for eight Formators. Further, memory increment (x2, x4) is on the scope and depends of availability of higher than 128 Gigabit density FLASH-memory chips in planar cases.

6. DATA TRANSFER TO EARTH

The data should be transferred from the L2 orbit (1.5 – 1.75 million km) to Earth. Obviously, this part of the S-E VLBI interferometer system is a bottleneck because of the potential huge number of data to be transferred to the correlator located at the ground.

6.1 Basic solution

The system transferring the scientific data from Formator to Earth is planned to be based on a radio line operating at frequency 15 GHz and providing 1.2 GBit/sec data rate. The long distance and a lack of the onboard power are limiting the signal to noise ratio. Relatively low carrier frequency puts restrictions to the available bandwidth. Moreover, the antenna gain goes down for the lower frequency.

6.2 Possibility towards increasing the speed of data transmission in broadband millimeter-wave channels

The most prospective way to increase the data rate is to use a higher carrier frequency, particularly E-band (71-76; 81-86 GHz). High gain of the antenna allows to transmit data with a high noise immunity. Going into details, the transmitter power at L2 can be 200 W. At the same time, the receiver noise power can be estimated as $7 \cdot 10^{-11}$ W for a receiver with a following parameters: a) 5 GHz frequency band, b) physical temperature of 50K, c) noise figure of 3 dB. The gains at a frequency of 75 GHz with transmitting and receiving antenna diameters of 2 and 15 m will be 60.7 and 78.2 dB, respectively. The choice of the E-band is due, on the one hand, to the relatively low value of the zenith attenuation of the signal [16], and on the other hand, the higher gain of the antennas in comparison with the lower millimeter-wave frequencies (30–40 GHz). Finally, the 10 GHz bandwidth of the E-band allows the transmission of simplex data with QPSK modulation at rate of 20 Gbit/s without signal coding and 16-18 Gbit/s with signal coding.

6.3 Improving the budget of a space communication channel using error-correcting coding

Deep space radiation causes degradation of the onboard memory. This brings errors in the scientific data. Those errors could be corrected in a normal case, but in case of overlap with the data transfer (channel) errors we have uncorrectable errors in the channel decoder. To mitigate this risk, we are considering implementation of the switchable error-correcting module based on additional onboard coder. Corresponding decoder will be applied on the ground.

1. It is advisable to apply double independent coding. Firstly, utilizing a memory coding to correct errors when writing/reading data to/from Formator memory to Highly Informative Radio-engineering Complex (HIRC). Here, the memory encoder is made in the onboard version and is located respectively in the satellite, and the memory decoder is presented in two versions: ground and onboard, located respectively on the Ground Tracking Station (GTS), after the channel decoder and onboard the Millimetron, between the memory output of the Formator and HIRC. Secondly, using channel (noise-immune) coding for error correction in the Millimetron channel - GTS (HIRC channel). For this encoding, the encoder is placed onboard Millimetron, the decoder is put on the GTS.

2. At the first stage of work, it is advisable to encode data using onboard memory encoder when writing them to the Formator's memory, transfer them from memory without decoding to the HIRC channel, where error-correcting coding will be implemented to correct errors in the communication channel. On GTS at first must perform channel decoding and then use non board the memory decoder (use the GTS memory decoder) to decode the data to correct errors emerging in the memory of the onboard Formator. Data errors in the Formator's memory during the initial period of operation will be insignificant and therefore their influence on data errors in the HIRC channel is negligible (Fig. 6).

3. In the future, as the memory elements of the Formator degrade, the errors that occur there will be significant. At the same time, they will accordingly have a great impact on the functioning of the HIRC encoder / decoder, which can lead to a significant increase in errors and loss of scientific data transmission reliability.

4. To prevent this and increase the time resource for the operation of the Millimetron mission, it is advisable to decode errors from the memory aboard Millimetron with an appropriate memory decoder. That is, turn off the memory decoder in GTS and switch the operation to the memory onboard decoder located on the Millimetron, between the memory output of Formator and HIRC. In this case, HIRC will receive more cleared (from errors) data, the channel encoder / decoder will work in the normal mode. It is expedient to turn on the onboard data decoder from the Formator memory only when a certain error threshold is accumulated, which is determined in advance, when the normal (standard) operation of HIRC channel encoder/decoder becomes unacceptable (Fig. 7).

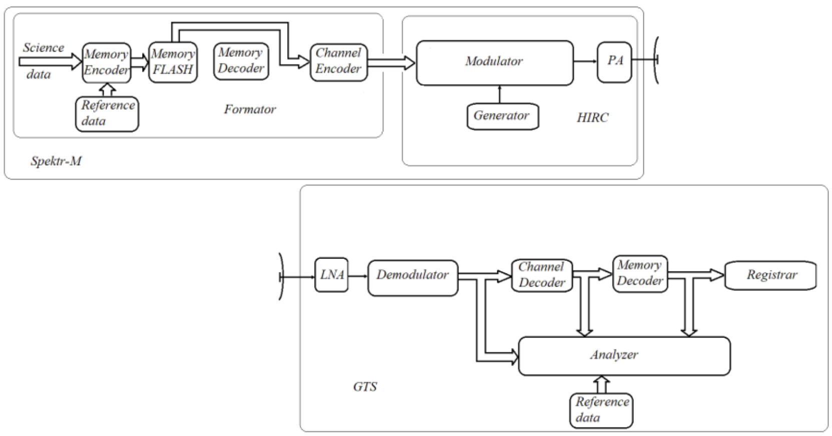

Figure 6. Circuit operation with small memory errors.

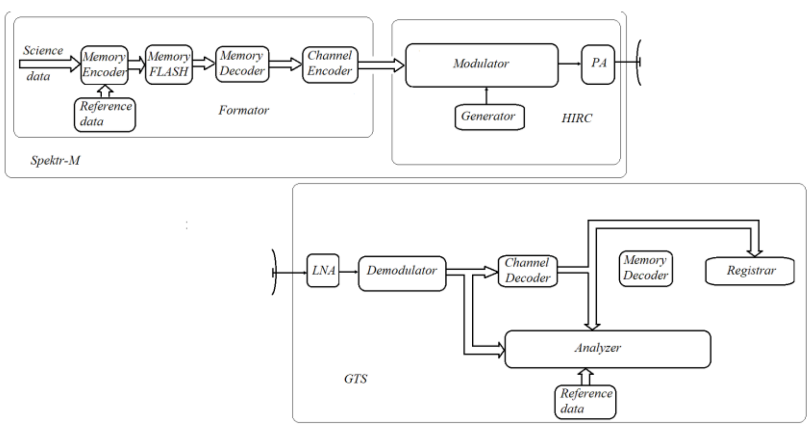

Figure 7. Circuit operation with a high number of memory errors.

5. In order to be able to correct group packets of errors that may occur in the event of a failure of Formator memory elements, it is advisable to use non-redundant interleaving codes [17]. The use of this type of codes is possible to improve the reliability of the Formator's electronic memory elements.

6. In addition, the use of codes of this type allows, in a certain established order, to exclude part of the memory elements in operation without losing the total amount of data. For channel coding, it is advisable to use random codes or

high speed RS codes. The interleaved (NxM) code must have a length (N or M) greater than the memory capacity of the exception element. The interleaving can be realized both according to the standard periodic law and according to the pseudo-random law [17]. The interleaved code transforms burst errors into single ones, which are easily corrected by redundant (random or RS codes).

For channel coding, it is advisable to consider random cod**es:** LDPS (Low Density Parity Check) or polar codes with high corrective power [18].

ACKNOWLEDGEMENTS

Fabrication of the Nb-AlOx –Nb junctions was carried out by the USU “Cryointegral” at Kotelnikov IRE RAS, USU is supported by a grant from the Ministry of Science and Higher Education of the Russian Federation, agreement No. 075-15-2021-667.

REFERENCES

[1] Kardashev, N.S., Khartov, V.V., Abramov, V.V. *et al.* “RadioAstron”-A telescope with a size of 300 000 km: Main parameters and first observational results., Astron. Rep. 57, 153–194 (2013).
[2] The Event Horizon Telescope Collaboration, First M87 Event Horizon Telescope Results. II. Array and Instrumentation, The Astrophysical Journal Letters 875 (L2) (2019).
[3] The Event Horizon Telescope Collaboration,First M87 Event Horizon Telescope Results. III. Data Processing and Calibration, The Astrophysical Journal Letters 875 (L3) (2019).
[4] Likhachev, S. F., Rudnitskiy, A. G., Shchurov, M. A., Andrianov, A. S., Baryshev, A. M., Chernov, S. V., Kostenko, V. I., “High-resolution imaging of a black hole shadow with Millimetron orbit around lagrange point l2”, Monthly Notices of the Royal Astronomical Society, 511 (1), 668–682 (2022).
[5] Raymond, A.W., Palumbo, D., et al., “Evaluation of New Submillimeter VLBI Sites for the Event Horizon Telescope”, The Astrophysical Journal Supplement Series 253 (1), 5, (2021).
[6] Koshelets, V., Rudakov, K., Khudchenko, A. et al. Superconducting Sub-THz Receivers for Space and Ground-Based Radio Astronomy. Bull. Lebedev Phys. Inst. 48, 287–291 (2021).
[7] Rudakov, K.I., Dmitriev, P.N., Baryshev, A.M. , A. M., Khudchenko, A. V., Hesper, R., & Koshelets, V. P. , “Low-Noise Sis Receivers for New Radio-Astronomy Projects”, Radiophysics and Quantum Electronics, vol. 62, No. 7, 547–555 (2019).
[8] Kerr, A.R., Pan, S.-K., Claude, S.M.X., et al., “Development of the ALMA Band-3 and Band-6 sideband-separating SIS mixers”, IEEE Trans. THz Sci. Technol., vol. 4, p. 20 (2014).
[9] ALMA Cycle 8, 2021, Technical Handbook, Doc 8.5, ver. 1.0, 15 March, 2021.
[10] L. Blackburn, S. Doeleman et al.,Studying Black Holes on Horizon Scales with VLBI Ground Arrays., arXiv:1909.01411v2, (2019).
[11] Zhao, G.-Y., et al. "The power of simultaneous multi-frequency observations for mm-VLBI: beyond frequency phase transfer." The Astronomical Journal, 155(1), 26 (2017).
[12] Water Vapor Radiometry at ALMA: Properties of the Atmosphere and First Tests of Phase Correction, B. Nikolic, R. Bolton & J. S. Richer, Cavendish Laboratory/Kavli Institute,University of Cambridge 8 March 2011
[13] Jung, T., et al. "First Simultaneous Dual-Frequency Phase Referencing VLBI Observation with VERA." Publications of the Astronomical Society of Japan, 63(2), 375-385 (2011).
[14] Rioja, M.J., et al. "Exploration of source frequency phase referencing techniques for astrometry and observations of weak sources with high frequency space very long baseline interferometry." The Astronomical Journal, 142(5), 157, (2011).
[15] Rioja, M.J., et al. "The power of simultaneous multi-frequency observations for mm-VLBI: Astrometry up to 130 GHz with the KVN." The Astronomical Journal 150(6), 202 (2015).
[16] ITU-R Recommendation R.676-10 (09/2013).
[17] Clark, G.C., Jr. and Cain, J.B., “Error Correction Coding for Digital Communications”, New York: Springer, 1981.
[18] Moon, T.K., “Error Correction Coding”, Wiley Interscience, P. 751 (2005)